Journal of Inorganic Biochemistry 194 (2019) 19–25

Contents lists available at ScienceDirect

Journal of Inorganic Biochemistry

journal homepage: www.elsevier.com/locate/jinorgbio

Design of ruthenium-albumin hydrogel for cancer therapeutics and luminescent imaging

Zhiquan Zhao[a], Rentao Hu[a], Hongdong Shi[a], Yi Wang[a], Liangnian Ji[b], Pingyu Zhang[a,*], Qianling Zhang[a,*]

[a] Department of Chemistry and Environmental Engineering, Shenzhen University, Shenzhen 518060, PR China
[b] Department of Chemistry, Sun Yat-sen University, Guangzhou 510275, PR China

ARTICLE INFO

Keywords:
Ruthenium
Albumin
Hydrogel
Therapy
Imaging

ABSTRACT

Improving cell uptake of metal compounds has became an important goal in the field of metal-based anticancer agents. This may combat platinum resistance and side effects seen commonly in current anticancer chemotherapy regimes. Here, we explore a novel degradable ruthenium-albumin hydrogel, which shows strong luminescence for cell imaging and high selectivity for cancer cells *versus* non-cancer cells. This is an early indication of the possibility of reducing unwanted side effects of metals by using bovine serum albumin hydrogel as a delivery strategy. This work provides a strong basis for development of a new class of metal-based cancer therapeutic agents.

1. Introduction

Hydrogels are three-dimensional networks of hydrophilic natural or synthetic polymers [1–4]. Due to their high-water content, tissue-mimic physical and mechanical properties and biocompatibility, hydrogels have the potency to be used in numerous biomedical applications such as tissue repair [5], sensing [6,7], reconstructive surgery [8,9] and drug delivery [10–12]. Protein based hydrogel materials are promising in various biomedical applications because of their biocompatibility and viscoelasticity with the advantage being their easy degradability in the body [13–15]. Hydrogels made of bovine serum albumin (BSA) have been extensively studied due to its good solubility, low cost and excellent ligand binding accessibility and intrinsic emission properties [16–19].

Metal coordination complexes have attracted a great interest in the fields of chemical sensors, chemotherapeutic agents and bioimaging because they possess great biocompatibility, tuneable and intense emission and long emission lifetimes [20–29]. However, there was only one example of metal-based hydrogel that Peter J. Sadler et al. reported a biocompatible platinum (IV)-G-quartets hydrogel as photoactivatable prodrug for cancer therapy [30].

Conjugates of albumin can be effective for delivery of anticancer drugs. Albumin contains a free thiol residue at cysteine-34, is abundant in blood serum (*ca.*0.6 mM), rich in histidine [31], a physiological antioxidant [32], and binds a wide range of biologically and clinically important molecules [33–35]. The effectiveness of albumin-coupled anticancer drugs has been established clinically for doxorubicin (INNO206; aldoxorubicin) [36], and albumin-based nanoparticle-encapsulated paclitaxel (Abraxane®) [37]. Recently, albumin-functionalized metal complexes have been developed for cancer therapy, and illustrate that a key role can be played by albumin in augmenting anticancer activity [38–41].

In the previous research, scientists proposed an amount of Ru(II) polypyridyl complexes for cancer therapy and luminescent imaging [42–46]. Although both luminescent polypyridyl Ru complexes and BSA hydrogels alone had been widely studied, to the best of our knowledge, luminescent ruthenium-bovine serum albumin hydrogel (Ru-BSA hydrogel) for cell imaging and cancer therapy has not been studied in literature yet. The strategy to prepare metal-BSA hydrogel could significantly expand the scope of hydrogels and metal-based agents in biomedical applications.

In this study, we designed a novel Ru-BSA hydrogel, which was a degradable material in biological system. The Ru-BSA hydrogel exhibited strong luminescence and was used for cell imaging. Interestingly, we observed that the green luminescence in the lysosome was from BSA of the degraded Ru-BSA hydrogel, and the red luminescence in the mitochondria was from the released Ru complex of the degraded Ru-BSA hydrogel. The result meant that the Ru complex could be released after Ru-BSA degradation in the living cells. Furthermore, the Ru-BSA hydrogel exhibited greatly enhanced anti-cancer activity

* Corresponding authors.
E-mail addresses: p.zhang6@szu.edu.cn (P. Zhang), zhql@szu.edu.cn (Q. Zhang).

https://doi.org/10.1016/j.jinorgbio.2019.02.002
Received 3 November 2018; Received in revised form 26 January 2019; Accepted 3 February 2019
Available online 10 February 2019
0162-0134/

compared to the bare Ru complex and high selectivity for cancer cells *versus* normal cells. This work developed a strategy to study Ru-BSA hydrogel as a novel metal-based agent for cancer therapy.

2. Materials and methods

2.1. Materials

BSA is purchased from Sigma-Aldrich. Its concentration was measured by absorption method (the concentration was calculated by A_{280}/36850, 1 cm curve). 3-(4,5-dimethylthiazol-2-yl)-2,5-diphenyltetrazolium bromide (MTT) and glutaraldehyde solution (25%, v/v) were purchased from Alfa Aesar. The liver hepatocellular carcinoma (Hep-G2) cell line and liver normal cell line (LO2) were purchased from Sigma-Aldrich. Roswell Park Memorial Institute medium (RPMI-1640), fetal calf serum (FCS), glutamine and penicillin/streptomycin were purchased from Sigma-Aldrich.

2.2. Instruments

UV–visible absorption spectra were recorded on a Varian Cary 300 UV–vis spectrophotometer. The fluorescent spectra were measured on JASCO FP-6500 Fluorimeter. The confocal images were visualized using Zeiss 710 confocal microscopy (63 × oil-immersion objective). Surface morphology of the prepared hydrogel was studied using JEOL 6335 Scanning Electron Microscope (SEM) operated at an accelerating voltage of 10 kV and 12 μA.

2.3. Synthesis of BSA and Ru-BSA hydrogel

Synthesis of BSA hydrogel: 4 mL BSA (5 mg/mL in water) and 210 μL glutaraldehyde solution (25%; v/v) were mixed quickly. The final glutaraldehyde concentration was 1% (v/v). After 10 s, BSA hydrogel was prepared. ***Synthesis of Ru-BSA hydrogel***: The ruthenium complex (1.2 mg/mL in water, 1 mL) and BSA (5 mg/mL in water, 4 mL) were mixed and then 210 μL glutaraldehyde solution (25%; v/v) was added into the mixture solution as a cross-linker. The clear orange Ru-BSA hydrogel which did not flow upon inversion, was obtained within 50 s. The hydrogel was further dialyzed with 8000 Da bag filter to remove the free ruthenium complex and redundant glutaraldehyde molecule. The Ru content of Ru-BSA hydrogel was measured by inductively coupled plasma optical emission spectrometer (ICP-OES) (Thermo Elemental Co., Ltd). The stock solution of BSA hydrogel was 20 mg/mL. The BSA concentration and Ru complex concentration of Ru-BSA hydrogel were 20 mg/mL and 1.0 mg/mL, respectively.

2.4. In vitro enzymatic biodegradation test

In vitro degradation test was conducted in a small glass vial containing 400 μg/mL BSA hydrogel or Ru-BSA hydrogel ([Ru complex] = 20 μg/mL; [BSA hydrogel] = 400 μg/mL) and 5 mL of PBS buffer (pH 7.4 10 mM) with 1 mg/mL proteinase K. The pictures were recorded at different time intervals (0 h, 1 h, 2 h, 4 h, 12 h and 24 h). After 5000*g* centrifugation for 30 min, the Ru complex contents in the solution were measured by ICP-OES.

2.5. Cellular imaging

The cells were incubated with BSA hydrogel or Ru-BSA hydrogel ([Ru complex] = 20 μg/mL; [BSA hydrogel] = 400 μg/mL) at 37 °C for 4 h and then co-stained with 500 nM LysoTracker®Red or MitoTracker®Green for 30 min. The cells were then washed three times with PBS and visualized using Zeiss 710 confocal microscopy (63 × oil-immersion objective). The excitation and emission wavelengths for Ru-BSA: λ_{ex} = 488 nm, λ_{em} = 600 ± 30 nm or λ_{ex} = 405 nm, λ_{em} = 500 ± 30 nm; LysoTracker® Red: λ_{ex} = 563 nm, λ_{em} = 595 ± 30 nm. MitoTracker® Green: λ_{ex} = 488 nm, λ_{em} = 520 ± 30 nm.

2.6. ICP-OES analysis

Exponentially grown Hep-G2 cells were incubated with the Ru complex or Ru-BSA hydrogel ([Ru complex] = 20 μg/mL; [BSA hydrogel] = 400 μg/mL) for varying amounts of time at 37 °C. After digestion, the cells were counted and divided into two portions. In the first portion, the lysosome was extracted using a lysosome extraction kit (Promega); in the second portion, the mitochondria were extracted using a mitochondrial extraction kit (Promega). The samples were digested with 60% HNO_3 at RT for 72 h. Each sample was diluted with Milli-Q H_2O to obtain 2% HNO_3 sample solutions. The ruthenium complex concentrations were determined using ICP-OES.

2.7. Cytotoxicity test

The cytotoxicity test was determined towards the Hep-G2 and LO2 cells. The cells were grown in RPMI-1640 according to the protocol below. All media were supplemented with 10% v/v of FCS, 1% v/v of 2 mM glutamine and 1% v/v penicillin/streptomycin. All cells were grown as adherent monolayers at 310 K in a 5% CO_2 humidified incubator and passaged regularly at approx. 80% confluence. Approximately 5×10^3 cells/well were seeded into 96-well plates, followed by 24 h incubation for attachment. The cells were then exposed to the hydrogels with different concentrations ([Ru complex] = 0–100 μg/mL; [BSA hydrogel] = 0–2000 μg/mL). After 48 h incubation, the cytotoxicity was measured by standard MTT method. The change in optical density (OD) at 490 nm was monitored using microplate reader (Promega).

3. Results and discussion

3.1. Synthesis of Ru-BSA hydrogel

The synthesis of the ruthenium polypyridine saturated coordination complex was described in our previous report [47]. It had been characterized using the MS, NMR and elemental analysis. We had studied that the Ru complex showed MLCT absorption at 459 nm and red phosphorescence from 550 to 700 nm. It was hydrophilic with a log P of −2.23 and mainly accumulated in mitochondria in the living lung cancer cells. It exhibited no cytotoxicity (IC_{50} = 425 μM) in the dark after 4 h treatment. However, it was highly toxic to A549 cancer cells (IC_{50} = 12.3 μM) after 465 nm blue light irradiation but not after 633 nm red light irradiation (IC_{50} = 442 μM). Due to its poor dark cytotoxicity, we here use BSA hydrogel to deliver the ruthenium complex to cancer cells and enhance its anticancer activity.

The Ru-BSA hydrogel was synthesized by a simple and rapid method, which was showed in the experiment section. Briefly, the ruthenium complex and BSA were dissolved in water and then glutaraldehyde was added into the mixture solution as a cross-linker. Glutaraldehyde predominantly crosslinks ε-amino groups of lysine within BSA [48]. After that, a clear orange hydrogel was obtained within 50 s. The hydrogel was further dialyzed with 8000 Da bag filter to remove the free ruthenium complex and redundant glutaraldehyde molecule. ICP-OES study showed that the concentration of Ru complex of Ru-BSA hydrogel was 1 mg in 20 mg BSA hydrogel. The schematic representation of the Ru-BSA hydrogel was presented in Fig. 1.

3.2. Characterization of Ru-BSA hydrogel

We firstly studied the UV–vis spectra of Ru-BSA hydrogel, as shown in Fig. S1. Both BSA hydrogel and Ru-BSA hydrogel exhibited absorption in a broad wavelength range (400–800 nm) compared to BSA solution and Ru complex solution. And there was an obvious absorption of Ru-BSA hydrogel at ~460 nm, which was assigned to the Ru complex.

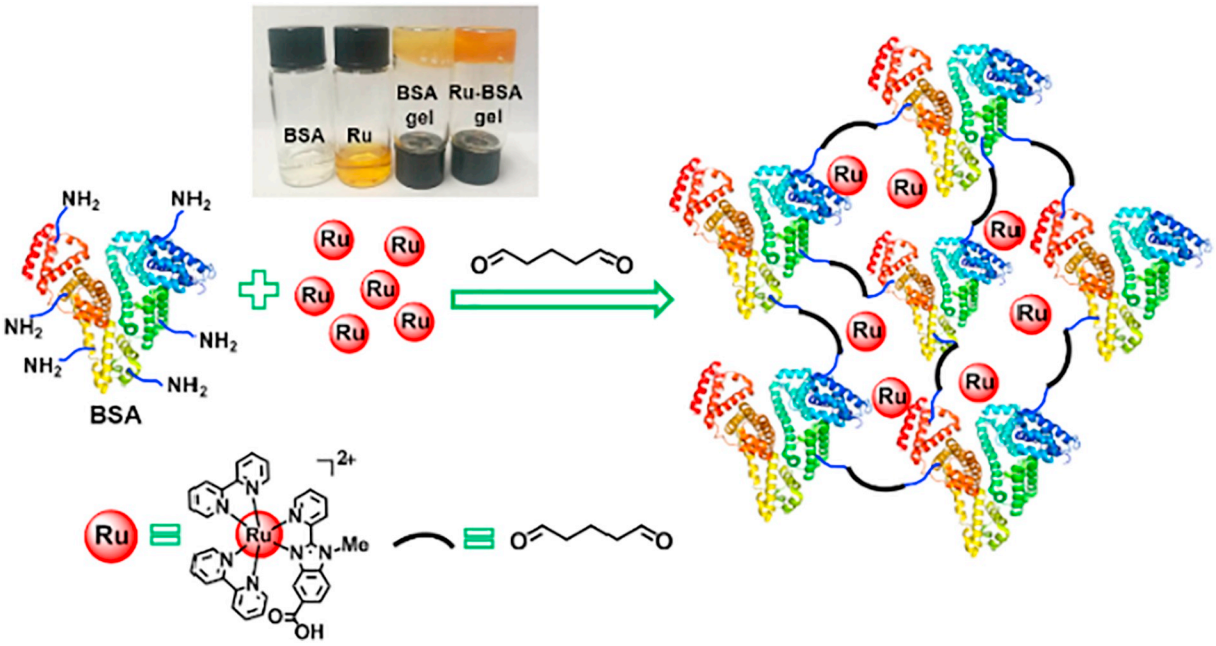

Fig. 1. The schematic diagram of the Ru-BSA hydrogel. The inserted vials were photographed under white light.

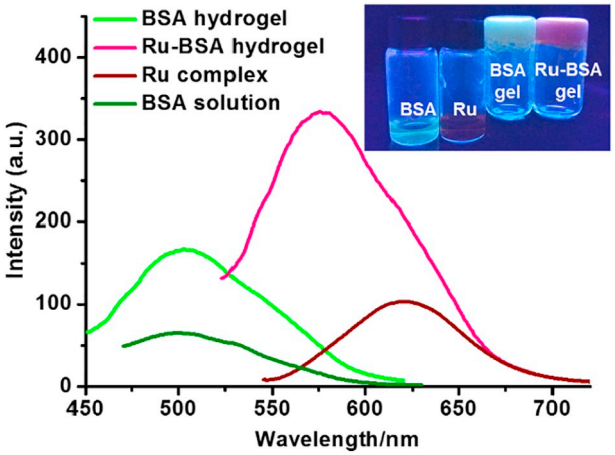

Fig. 2. The emission spectra of BSA (400 μg/mL), Ru complex (20 μg/mL), BSA hydrogel (400 μg/mL) and Ru-BSA hydrogel ([BSA] = 400 μg/mL; [Ru complex] = 20 μg/mL), respectively; the wavelength of excitation was 488 nm. The inserted vials were photographed under UV light irradiation.

Then the luminescent spectra were acquired upon 488 nm excitation. As shown in Fig. 2. BSA hydrogel exhibited green emission between 450 and 550 nm. In contrast, Ru-BSA hydrogel showed strong red luminescence with the wavelength of emission between 550 and 650 nm. We further observed that the Ru-BSA hydrogel exhibited green and red emission upon 405 nm and 488 nm excitation, respectively (Fig. S2). This is probably the green emission upon 405 nm excitation was mainly from the BSA and the red emission upon 488 nm excitation was from the Ru complex. In addition, the maximum emission wavelength of Ru-BSA hydrogel gradually red-shifted from 550 nm to 602 nm along with increasing the ratios of the ruthenium complex in Ru-BSA hydrogel (Fig. S3). These results meant that the emission of Ru-BSA hydrogel red-shifted dramatically compare to the BSA hydrogel. This is probably due to the red emission of the Ru complex.

To characterize the morphology of the Ru-BSA hydrogel, SEM measurements were employed. Both BSA hydrogel and Ru-BSA hydrogel exhibited a highly porous honeycomb-like structure with an irregular shape in which the three-dimensional, interconnected macropores represent water-filled areas (Fig. S4). The BSA hydrogel was characterized with an average pore size of 1.2 μm. The Ru-BSA hydrogel exhibited a bigger pore size of 3.4 μm. The results mean that the ruthenium complex joining in the BSA hydrogel can enlarge the pore size. It is possible that the ruthenium complex occupied in the cavities of BSA hydrogel. In addition, the ruthenium complex is positive charge and the BSA hydrogel is negative charge. There is also probably an electrostatic interaction between them.

3.3. *In vitro* enzymatic degradation of Ru-BSA hydrogel

As it is difficult to remove the unreacted residues after injection and curing, biodegrability is one of the most important factors to evaluate the merits of hydrogels [49]. The *in vitro* biodegradability of Ru-BSA hydrogel was tested *via* proteinase K method [50]. Proteinase K is a widely used enzyme for protein digestion, because it can hydrolyze the amide bonds and also break ester bonds. As shown in Fig. 3a, the Ru-BSA hydrogel was digested by increasing digestion time (0–24 h) at 37 °C. The colour changes of the solution during the digestion process were observed obviously, and then the concentrations of Ru contents in the solution were measured by ICP-OES (Fig. 3b), indicating that the ruthenium complex was released gradually by increasing digestion time. We also measured the MS spectrum of the released complex in the solution after proteinase K digestion. The result showed that the whole Ru complex (*m/z* 666.1) was unabridged (Fig. S5).

3.4. Cellular location of Ru-BSA hydrogel

We dispersed the Ru-BSA hydrogel in PBS solution for *in vitro* experiment. The particles size of the gel was 59 ± 6 nm. This result was showed in Fig. S6 and it was highly stability in the PBS solution for 72 h. Due to the luminescence property of Ru-BSA hydrogel, its distribution in the living cells was investigated using confocal laser scanning microscopy. The images were collected under two different

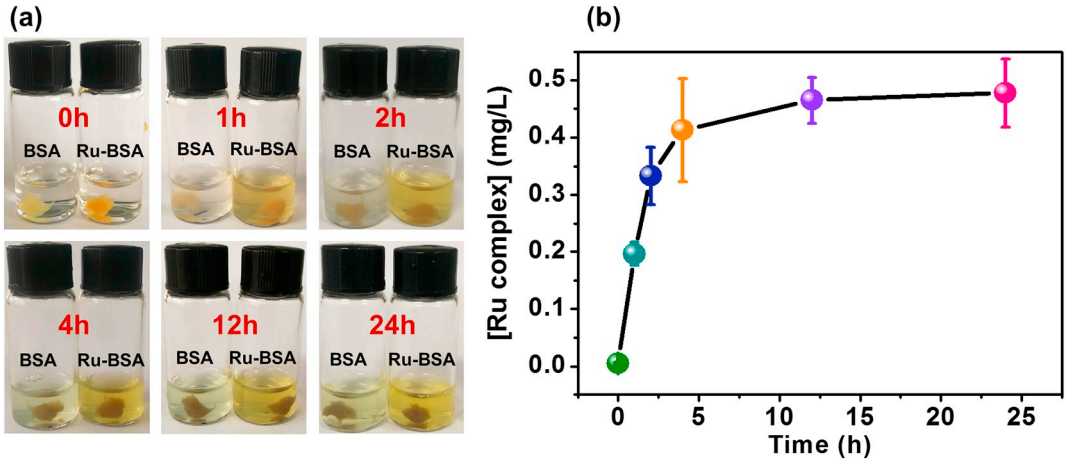

Fig. 3. (a) The Ru-BSA hydrogel (m(BSA hydrogel) = 10 mg; m(Ru complex) = 0.5 mg) and BSA hydrogel (10 mg) were digested in 1 mL proteinase K (1 mg/mL) solution with increasing digestion time. (b) The Ru complex concentrations at each time were measured by ICP-OES.

excitation channels (λ_{ex} = 405 nm and λ_{ex} = 488 nm). As shown in Fig. 4a–b, the green luminescence images were observed upon 405 nm laser excitation, whereas no red luminescence was observed. However, upon 488 nm laser excitation, strong red luminescence was observed in the cells. Most interestingly, the green and red luminescence in the cells showed in the different location.

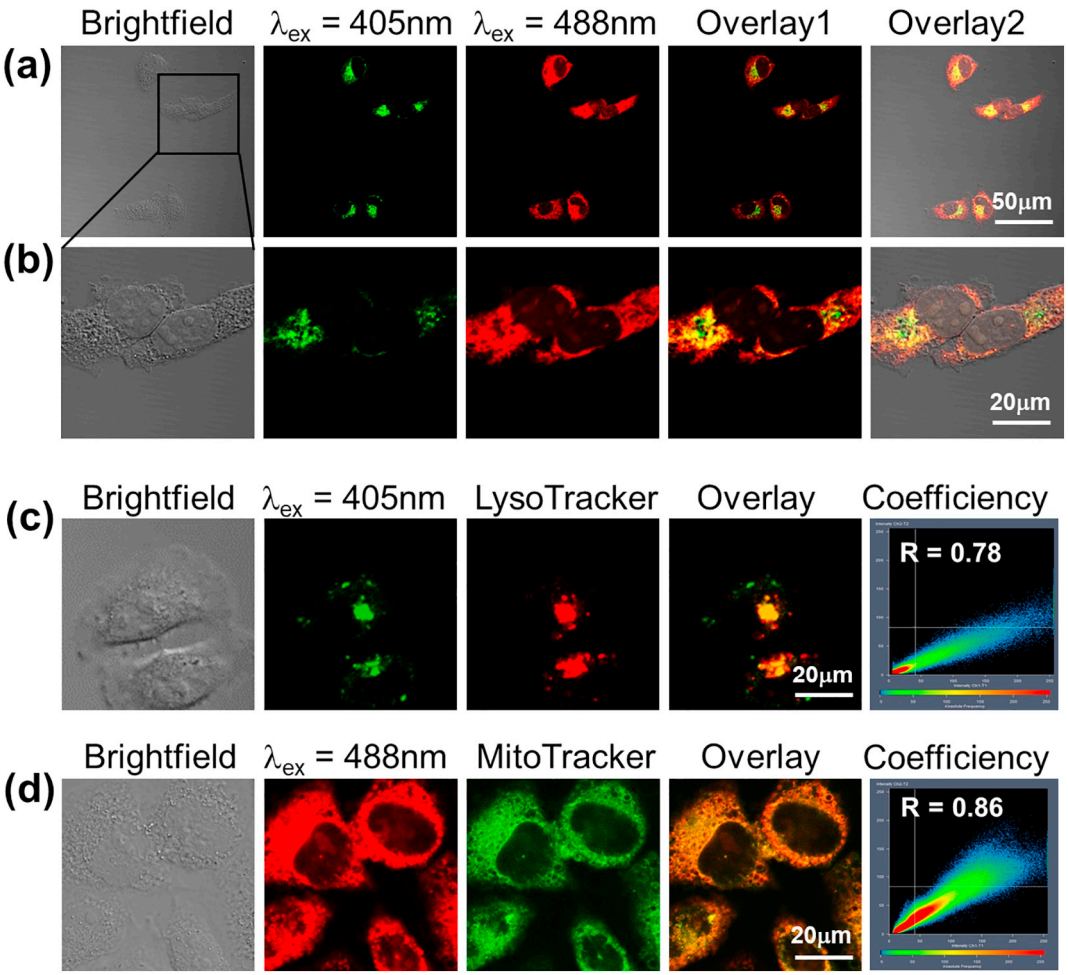

Fig. 4. (a) Confocal microscopy images of the living Hep-G2 cells incubated with Ru-BSA hydrogel ([Ru complex] = 20 μg/mL; [BSA hydrogel] = 400 μg/mL, 4 h); (b) is the enlarge view in (a); (c) confocal microscopy images of the cells colabeled with Ru-BSA hydrogel and LysoTracker®Green (500 nM, 30 min); (d) confocal microscopy images of the cells colabeled with Ru-BSA hydrogel and MitoTracker®Red (500 nM, 30 min); Ru-BSA: λ_{ex} = 405 nm, λ_{em} = 500 ± 30 nm or λ_{ex} = 488 nm, λ_{em} = 600 ± 30 nm; LysoTracker®Red: λ_{ex} = 563 nm, λ_{em} = 595 ± 30 nm; MitoTracker®Green: λ_{ex} = 488 nm, λ_{em} = 520 ± 30 nm.

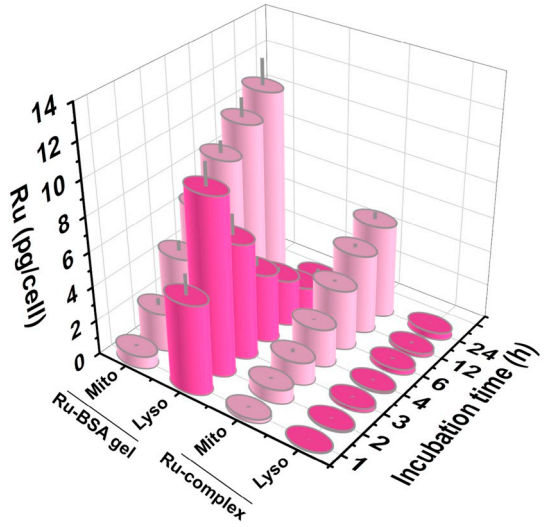

Fig. 5. Ruthenium concentrations determined in lysosome and mitochondria of the Hep-G2 cells with exposure to the ruthenium complex or Ru-BSA hydrogel ([Ru complex] = 20 μg/mL) for 1–24 h by ICP-OES.

To investigate its specific sub-cellular location, the colocation experiments with organelle commercial dyes were further studied. As shown in Fig. 4c–d, the results demonstrated the green luminescence of Ru-BSA hydrogel located in the lysosome with a Pearson's colocalization coefficient of 78%. Whereas, the red luminescence of Ru-BSA hydrogel accumulated in the mitochondria with a Pearson's colocalization coefficient of 86%. We speculated that the Ru-BSA hydrogel firstly entered the cells *via* endocytosis (because green luminescence of Ru-BSA hydrogel showed in lysosome), then the Ru-BSA hydrogel was degraded by the enzymes in the cells, finally the ruthenium complex was released and accumulated in the mitochondria. As we had reported the bare Ru complex accumulated in the mitochondria [47]. The pure BSA hydrogel was found to locate throughout the whole cells (Fig. S7). These results suggested that the Ru-BSA hydrogel was degradable and the Ru complex could be released in the living cells.

The amounts of Ru complex in lysosome and mitochondria of the cells were quantitatively determined using ICP-OES. The Hep-G2 cells were exposed to the Ru complex or Ru-BSA hydrogel at a concentration of 20 μg/mL (The concentration was based on Ru complex) after 1–24 h incubation. As shown in Fig. 5, in the short time incubation (1 h and 2 h), the Ru contents of Ru-BSA hydrogel were mainly accumulated in the lysosome but not mitochondria. However, by increasing the incubation time (3–24 h), we observed that more and more Ru complexes were in the mitochondria. These results prove our speculation, that is, the Ru-BSA hydrogel firstly enters the cells *via* endocytosis, then is degraded by the enzymes in the cells, finally the ruthenium complex is released and accumulates in the mitochondria.

3.5. Cytotoxicity of Ru-BSA hydrogel

The cytotoxicities of Ru complex, BSA hydrogel and Ru-BSA hydrogel towards liver cancer (Hep-G2) and liver normal (LO2) cells were further studied. The result showed that BSA solution or BSA hydrogel showed almost no cytotoxicity (the cell viabilities were all above 90% at all concentrations) towards both Hep-G2 and LO2 (Fig. S8) and the IC_{50} values of the Ru complex towards Hep-G2 and LO2 were approximately 100 μg/mL. However, Ru-BSA hydrogel was highly toxic towards Hep-G2 cancer cells (IC_{50} = 15.6 ± 1.3 μg/mL) but not normal liver LO2 cells (IC_{50} = 106.2 ± 4.6 μg/mL) (Fig. 6). The results indicated that the Ru-BSA hydrogel enhanced anti-cancer activity compared to bare ruthenium complex and exhibited high selectivity for cancer cells *versus* non-cancer cells.

As reported, BSA could be used as a drug carrier and designed to provide numerous gaps in the mesh to contain and carry a large number of drugs [51,52]. Furthermore, BSA is a natural polymer endowed with numerous advantages such as high safety, low immunogenicity, excellent biodegradability, good biocompatibility, facile modification, and availability at low cost [51,52]. In addition, BSA accumulates highly in activated cells, such as those in malignant tumour and inflamed tissues, to cover their increased need for amino acids and energy [53,54]. Here we also proved that BSA can enhance the cellular uptake ability of the ruthenium complex and improve the selectivity for tumour cells *versus* non-cancer cells.

4. Conclusions

In conclusion, we designed a metal-based BSA hydrogel for cell imaging and cancer therapy for the first time. The Ru-BSA hydrogel exhibited strong green and red luminescence, which could be clearly observed in the cells by confocal microscopy. Moreover, the Ru-BSA hydrogel was degraded in lysosome in the living cells and the Ru complex was released from the Ru-BSA hydrogel and accumulated in the mitochondria. Interestingly, incorporation of Ru complex into BSA hydrogel increased its cytotoxic potency towards Hep-G2 liver cancer cells and the selectivity between normal and cancer cells (~6.8-fold). This is an early indication of the possibility of reducing unwanted side

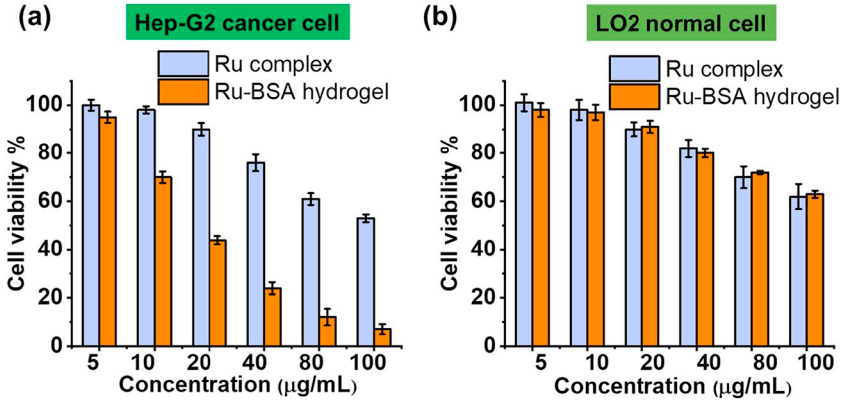

Fig. 6. The cell viabilities of Hep-G2 cancer cells and LO2 normal cells treated with different concentrations of the ruthenium complex and Ru-BSA hydrogel for 48 h, respectively. The concentrations were based on Ru complex.

effects by the use of the BSA hydrogel as a delivery strategy. Therefore, this strategy provides a strong basis for development of a new class of metal-based drugs as cancer therapeutic agents.

Abbreviations

BSA	bovine serum albumin
Ru-BSA	ruthenium-bovine serum albumin
ICP-OES	inductively coupled plasma-optical emission spectroscopy
SEM	scanning electron microscope
Hep-G2	human liver hepatocellular carcinoma cell line
LO2	human normal liver cell line
MTT	3-(4,5-dimethylthiazol-2-yl)-2,5-diphenyltetrazolium bromide
FCS	fetal calf serum
RPMI-1640	Roswell Park Memorial Institute medium
MLCT	Metal-to-Ligand Charge Transfer

Conflicts of interest

There are no conflicts to declare.

Acknowledgements

We appreciate the financial support of the National Natural Science Foundation of China (NSFC, 21701113 and 21671137), the Science and Technology Foundation of Shenzhen (JCYJ20170302144346218) and the Natural Science Foundation of SZU (2018036).

Appendix A. Supplementary data

Supplementary data to this article can be found online at https://doi.org/10.1016/j.jinorgbio.2019.02.002.

References

[1] R.G. Weiss, The past, present, and future of molecular gels. What is the status of the field, and where is it going? J. Am. Chem. Soc. 136 (2014) 7519–7530.
[2] S.S. Babu, V.K. Praveen, A. Ajayaghosh, Functional π-gelators and their applications, Chem. Rev. 114 (2014) 1973–2129.
[3] B. Li, K. Ren, Y. Wang, Y. Qi, X. Chen, Y. Huang, Protein-cross-linked hydrogels with tailored swelling and bioactivity performance: a comparative study, ACS Appl. Mater. Interfaces 8 (2016) 30788–30796.
[4] J.W. Steed, Anion-tuned supramolecular gels: a natural evolution from urea supramolecular chemistry, Chem. Soc. Rev. 39 (2010) 3686–3699.
[5] K.T. Nguyen, J.L. West, Photopolymerizable hydrogels for tissue engineering applications, Biomaterials 23 (2002) 4307–4314.
[6] C. Zhang, M.D. Losego, P.V. Braun, Hydrogel-based glucose sensors: effects of phenylboronic acid chemical structure on response, Chem. Mater. 25 (2013) 3239–3250.
[7] D. Zhai, B. Liu, Y. Shi, L. Pan, Y. Wang, W. Li, R. Zhang, G. Yu, Highly sensitive glucose sensor based on Pt nanoparticle/polyaniline hydrogel heterostructures, ACS Nano 7 (2013) 3540–3546.
[8] S. Közöl, E. Sawardecker, F. Teymour, V.H. Pérez-Luna, Sequential formation of covalently bonded hydrogel multilayers through surface initiated photopolymerization, Biomaterials 27 (2006) 1209–1215.
[9] X. Ma, J. Deng, Y. Du, X. Li, D. Fan, C. Zhu, J. Hui, P. Ma, W. Xue, A novel chitosan–collagen-based hydrogel for use as a dermal filler: initial in vitro and in vivo investigations, J. Mater. Chem. B 2 (2014) 2749–2763.
[10] T.R. Hoare, D.S. Kohane, Hydrogels in drug delivery: Progress and challenges, Polymer 49 (2008) 1993–2007.
[11] H. Ma, C. He, Y. Cheng, Z. Yang, J. Zang, J. Liu, X. Chen, Localized co-delivery of doxorubicin, cisplatin, and methotrexate by thermosensitive hydrogels for enhanced osteosarcoma treatment, ACS Appl. Mater. Interfaces 7 (2015) 27040–27048.
[12] X. Wu, C. He, Y. Wu, X. Chen, Synergistic therapeutic effects of Schiff's base cross-linked injectable hydrogels for local co-delivery of metformin and 5-fluorouracil in a mouse colon carcinoma model, Biomaterials 75 (2016) 148–162.
[13] Y. Gao, Q. Luo, S. Qiao, L. Wang, Z. Dong, J. Xu, J. Liu, Enzymetically regulating the self-healing of protein hydrogels with high healing efficiency, Angew. Chem. Int. Ed. 53 (2014) 9343–9346.
[14] Y. Sun, Y. Huang, Disulfide-crosslinked albumin hydrogels, J. Mater. Chem. B 4 (2016) 2768–2775.
[15] A.M. Jonker, D.W.P.M. Löwik, J.C.M. van-Hest, Peptide-and protein-based hydrogels, Chem. Mater. 24 (2012) 759–773.
[16] W. Qin, D. Ding, J. Liu, W.Z. Yuan, Y. Hu, B. Liu, B.Z. Tang, Biocompatible nanoparticles with aggregation-induced emission characteristics as far-red/near-infrared fluorescent bioprobes for in vitro and in vivo imaging applications, Adv. Funct. Mater. 22 (2012) 771–779.
[17] I.K. Deshapriya, B.S. Stromer, A. Pattammattel, C.S. Kim, R. Iglesias-Bartolome, L. Gonzalez-Fajardo, V. Patel, J.S. Gutkind, X. Lu, C.V. Kumar, Fluorescent, bioactive protein nanoparticles (prodots) for rapid, improved cellular uptake, Bioconjug. Chem. 26 (2015) 396–404.
[18] L.G. Naso, L. Lezama, M. Valcarcel, C. Salado, P. Villacé, D. Kortazar, E.G. Ferrer, P.A. Williams, Bovine serum albumin binding, antioxidant and anticancer properties of an oxidovanadium (IV) complex with luteolin, J. Inorg. Biochem. 157 (2016) 80–93.
[19] A. Upadhyay, R. Kandi, C.P. Rao, Injectable, self-healing, and stress sustainable hydrogel of BSA as a functional biocompatible material for controlled drug delivery in cancer cells, ACS Sustain. Chem. Eng. 6 (2018) 3321–3330.
[20] A. Notaro, G. Gasser, Monomeric and dimeric coordinatively saturated and substitutionally inert Ru(II) polypyridyl complexes as anticancer drug candidates, Chem. Soc. Rev. 46 (2017) 7317–7337.
[21] P. Zhang, C.K.C. Chiu, H. Huang, Y.P.Y. Lam, A. Habtemariam, T. Malcomson, M.J. Paterson, G.J. Clarkson, P.B. O'Connor, H. Chao, P.J. Sadler, Organoiridium photosensitizers induce specific oxidative attack on proteins within cancer cells, Angew. Chem. Int. Ed. 56 (2017) 14898–14902.
[22] M. Dickerson, Y. Sun, B. Howerton, E.C. Glazer, Modifying charge and hydrophilicity of simple Ru(II) polypyridyl complexes radically alters biological activities: old complexes, surprising new tricks, Inorg. Chem. 53 (2014) 10370–10377.
[23] L.J. Liu, W. Wang, S.Y. Huang, Y. Hong, G. Li, S. Lin, Z.W. Cai, H.M.D. Wang, D.L. Ma, C.H. Leung, Inhibition of the Ras/Raf interaction and repression of renal cancer xenografts in vivo by an enantiomeric iridium (III) metal-based compound, Chem. Sci. 8 (2017) 4756–4763.
[24] B. Pena, R. Barhoumi, R.C. Burghardt, C. Turro, K.R. Dunbar, Confocal fluorescence microscopy studies of a fluorophore-labeled dirhodium compound: visualizing metal–metal bonded molecules in lung cancer (A549) cells, J. Am. Chem. Soc. 136 (2014) 7861–7864.
[25] P. Zhang, H. Huang, Future potential of osmium complexes as anticancer drug candidates, photosensitizers and organelle-targeted probes, Dalton Trans. 47 (2018) 14841–14854.
[26] J.K. Barton, E.D. Olmon, P.A. Sontz, Metal complexes for DNA-mediated charge transport, Coord. Chem. Rev. 255 (2011) 619–634.
[27] S. Swavey, K. Morford, M. Tsao, K. Comfort, M.K. Kilroy, Heteroleptic monometallic and trimetallic ruthenium (II) complexes incorporating a π-extended dipyrrin ligand: light-activated reactions with the A549 lung cancer cell line, J. Inorg. Biochem. 175 (2017) 101–109.
[28] M.R. Gill, J.A. Thomas, Ruthenium (II) polypyridyl complexes and DNA—from structural probes to cellular imaging and therapeutics, Chem. Soc. Rev. 41 (2012) 3179–3192.
[29] H. Huang, B. Yu, P. Zhang, J. Huang, Y. Chen, G. Gasser, L.N. Ji, H. Chao, Highly charged ruthenium(II) polypyridyl complexes as lysosome-localized photosensitizers for two-photon photodynamic therapy, Angew. Chem. Int. Ed. 54 (2015) 14049–14052.
[30] V. Venkatesh, N.K. Mishra, I. Romero-Canelón, R.R. Vernooij, H. Shi, J.P. Coverdale, A. Habtemariam, S. Verma, P.J. Sadler, Supramolecular photoactivatable anticancer hydrogels, J. Am. Chem. Soc. 139 (2017) 5656–5659.
[31] X.M. He, D.C. Carter, Atomic structure and chemistry of human serum albumin, Nature 358 (1992) 209–215.
[32] R. Pirisino, P. Disimplicio, G. Ignesti, G. Bianchi, P. Barbera, Sulfhydryl groups and peroxidase-like activity of albumin as scavenger of organic peroxides, Pharmacol. Res. Commun. 20 (1988) 545–552.
[33] N. A. Malik, G. Otiko, P. J. Sadler, Control of intra-and extra-cellular sulphydryl-disulphide balances with gold phosphine drugs: 31P nuclear magnetic resonance studies of human blood, J. Inorg. Biochem. 12 (1980) 317–322.
[34] J.R. Roberts, J. Xiao, B. Schliesman, D.J. Parsons, C.F. Shaw, Kinetics and mechanism of the reaction between serum albumin and auranofin (and its isopropyl analogue) in vitro, Inorg. Chem. 35 (1996) 425–433.
[35] B.P. Esposito, R. Najjar, Interactions of antitumoral platinum-group metallodrugs with albumin, Coord. Chem. Rev. 232 (2002) 137–149.
[36] F. Kratz, INNO-206 (DOXO-EMCH), an albumin-binding prodrug of doxorubicin under development for phase II studies, Curr. Bioact. Compd. 7 (2011) 33–38.
[37] E. Miele, G.P. Spinelli, F. Tomao, S. Tomao, Albumin-bound formulation of paclitaxel (Abraxane® ABI-007) in the treatment of breast cancer, Int. J. Nanomedicine 4 (2009) 99–105.
[38] J. Mayr, P. Heffeter, D. Groza, L. Galvez, G. Koellensperger, A. Roller, B. Alte, M. Haider, W. Berger, C.R. Kowol, B.K. Keppler, An albumin-based tumor-targeted oxaliplatin prodrug with distinctly improved anticancer activity in vivo, Chem. Sci. 8 (2017) 2241–2250.
[39] Y.R. Zheng, K. Suntharalingam, T.C. Johnstone, H. Yoo, W. Lin, J.G. Brooks, S.J. Lippard, Pt (IV) prodrugs designed to bind non-covalently to human serum albumin for drug delivery, J. Am. Chem. Soc. 136 (2014) 8790–8798.
[40] M. Hanif, S. Moon, M.P. Sullivan, S. Movassaghi, M. Kubanik, D.C. Goldstone, T. Söhnel, S.M. Jamieson, C.G. Hartinger, Anticancer activity of Ru-and Os (arene) compounds of a maleimide-functionalized bioactive pyridinecarbothioamide ligand, J. Inorg. Biochem. 165 (2016) 100–107.
[41] S. Chakrabortty, B.K. Agrawalla, A. Stumper, N.M. Vegi, S. Fischer, C. Reichardt, M. Kögler, B. Dietzek, M. Feuring-Buske, C. Buske, S. Rau, Mitochondria targeted protein-ruthenium photosensitizer for efficient photodynamic applications, J. Am. Chem. Soc. 139 (2017) 2512–2519.
[42] N.A. Smith, P.Y. Zhang, S.E. Greenough, M.D. Horbury, G.J. Clarkson, D. McFeely,

A. Habtemariam, L. Salassa, V.G. Stavros, C.G. Dowson, P.J. Sadler, Combatting AMR: photoactivatable ruthenium (II)-isoniazid complex exhibits rapid selective antimycobacterial activity, Chem. Sci. 8 (2017) 395–404.
[43] S. Shi, X. Gao, J.L. Yao, H.L. Huang, J. Zhao, T.M. Yao, Effect of the ancillary ligands on the spectral properties and G-quadruplexes DNA binding behavior: a combined experimental and theoretical study, Chem. Eur. J. 21 (2015) 13390–13400.
[44] P. Zhang, Y. Wang, W. Huang, Z. Zhao, H. Li, H. Wang, C. He, Q. Zhang, "Turn off-on" phosphorescent sensor for biothiols based on a Ru-Cu ensemble, Sensors Actuators B Chem. 255 (2018) 283–289.
[45] Y. Wang, H.Y. Huang, Q.L. Zhang, P.Y. Zhang, Chirality in metal-based anticancer agents, Dalton Trans. 47 (2018) 4017–4026.
[46] P.Y. Zhang, P.J. Sadler, Advances in the design of organometallic anticancer complexes, J. Organomet. Chem. 839 (2017) 5–14.
[47] P.Y. Zhang, Y. Wang, K.Q. Qiu, Z.Q. Zhao, R.T. Hu, C.X. He, Q.L. Zhang, H. Chao, A NIR phosphorescent osmium (ii) complex as a lysosome tracking reagent and photodynamic therapeutic agent, Chem. Commun. 53 (2017) 12341–12344.
[48] A. Habeeb, R. Hiramoto, Reaction of proteins with glutaraldehyde, Arch. Biochem. Biophys. 126 (1968) 16–26.
[49] Z. Xie, Y. Zhang, L. Liu, H. Weng, R.P. Mason, L. Tang, K.T. Nguyen, J.T. Hsieh, J. Yang, Development of intrinsically photoluminescent and photostable polylactones, Adv. Mater. 26 (2014) 4491–4496.
[50] C. Zhao, X. Zhuang, H. Pan, C. Xiao, C. He, J. Sun, X. Chen, X. Jing, Synthesis of biodegradable thermo-and pH-responsive hydrogels for controlled drug release, Polymer 50 (2009) 4308–4316.
[51] H. Thakkar, R.K. Sharma, A.K. Mishra, K. Chuttani, R.R. Murthy, Albumin microspheres as carriers for the antiarthritic drug celecoxib, AAPS PharmSciTech 6 (2005) E65–E73.
[52] C. Du, D. Deng, L. Shan, S. Wan, J. Cao, J. Tian, S. Achilefu, Y. Gu, pH-triggered intracellular release from actively targeting polymer micelles, Biomaterials 34 (2013) 3087–3097.
[53] E. Neumann, E. Frei, D. Funk, M.D. Becker, H.H. Schrenk, U. Müller-Ladner, C. Fiehn, Native albumin for targeted drug delivery, Expert Opin. Drug Deliv. 7 (2010) 915–925.
[54] H. Shi, Q. Cheng, S. Yuan, X. Ding, Y.Z. Liu, Human serum albumin conjugated nanoparticles for pH and redox-responsive delivery of a prodrug of cisplatin, Chem. Eur. J. 21 (2015) 16547–16554.